Unsaturated Zone Hydrology for Scientists and Engineers

James A. Tindall, Ph.D.

United States Geological Survey, National Research Program
Department of Geography and Environmental Sciences, University of Colorado Denver

James R. Kunkel, Ph.D., P.E.

Knight Piésold, LLC, Denver, Colorado;
Department of Geology and Geological Engineering, Colorado School of Mines

with

Dean E. Anderson, Ph.D.

United States Geological Survey, National Research Program

PRENTICE HALL
Upper Saddle River, New Jersey 07458

12

Field Water in Soils

INTRODUCTION

Water and energy transport and retention processes are very complex in field soils. The soil is continually exposed to changes in water, heat, and chemical fluxes, both at and near the surface (Jury, Gardner, and Gardner 1991). Some of the material presented here was originally discussed in chapter 9; this chapter focuses on field water, radiation and energy balances, and provides practical methods to solve the water- and energy-balance equations from an applications or empirical point of view, as commonly used by many consulting and engineering firms in the United States and abroad.

Many of the techniques used to solve water-balance problems practically rely on empirical formulas, many of which use mixed units of English engineering, centimeter-gram-second (cgs) and Système International (SI). The units used in the source material for this chapter are preserved; this means that some formulas have English engineering units, whereas others have cgs or SI units. Conversions are given where appropriate, so that the results of the formulas can be presented in common units for a final water balance. For additional conversion factors, see the appendices.

12.1 FIELD WATER BALANCE

The general hydrologic equation describing the water balance of the unsaturated zone, from the soil surface to below the root zone, is given by (Thornthwaite and Mather 1955; 1957)

$$P - Q \pm \Delta S_w - E \pm \Delta S_s - D = 0 \tag{12.1}$$

where P is precipitation, Q is runoff, ΔS_w is change in storage of water ponded on the surface, E is evapotranspiration (evaporation plus transpiration), ΔS_s is change in soil-moisture storage, and D is deep percolation (unrecoverable by vegetation). Figure 12.1 shows each of these water-balance components in a schematic of the unsaturated zone. Water balances are used to evaluate and design water supply and water storage facilities for public and industrial uses as well as to evaluate environmental issues (Fenn, Hanley, and DeGeare 1975; van Zyl, Hutchinson, and Kiel 1988). When working with forests, interception (adherence of precipitation to the trunk, leaves, and stems of trees) of precipitation will occur. In such instances, interception, I, must become a variable of equation 12.1. For forests that have frequent, light precipitation, interception can account for as much as 50 percent of the precipitation. This intercepted precipitation does not fall to the ground and is not quickly evaporated into the atmosphere. Thus, equation 12.1 can be rewritten as $(P - I) - Q \pm \Delta S_w - E \pm \Delta S_s - D = 0$.

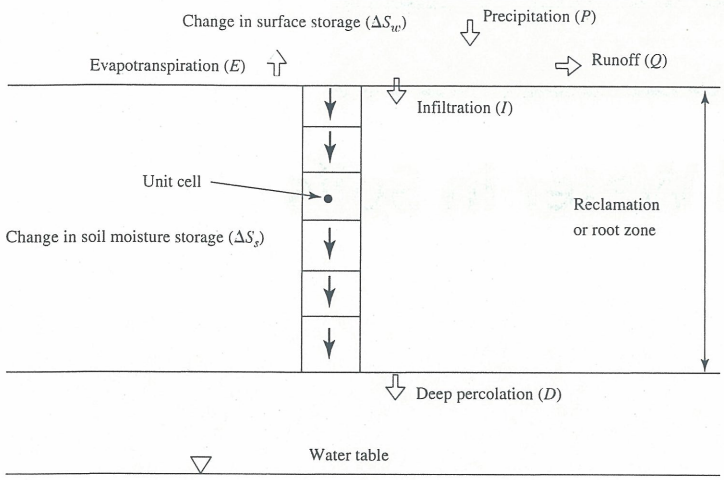

Figure 12.1 Schematic of water balance components (data from Kunkel and Murphy 1983)

Each of the terms in equation 12.1 represent inflows, outflows, or changes in storage over an arbitrary time period. All the water-balance terms in equation 12.1 are considered to be positive except the change in storage terms, which can be either positive or negative. Not all of the terms in equation 12.1 are computed directly. For example, infiltration is calculated as the difference between precipitation and runoff. Additionally, climatological variables, such as air temperature and solar radiation, are needed to calculate evapotranspiration. In general, deep percolation, D, is the unknown in equation 12.1 and can be determined by measuring or estimating the remaining terms.

The issue of what time increment to use in evaluating the individual terms in equation 12.1 is important. Obviously, all terms must be estimated using the same time increment: hour, day, month, or year. The question of whether a daily, monthly, or other time increment is used depends in part on the problem being solved, and the available data and estimation techniques. Most climatological data (precipitation, air temperature, evaporation, relative humidity, and solar radiation) are available on at least a daily basis throughout the world. However, sometimes only monthly summaries are published and easily obtainable, especially in developing countries. A general rule is to use the time increment that has the best available data. Often, an extreme event (such as the daily precipitation depth that falls, on the average, every 100 years) can be embedded into a more general time-series of daily precipitation values, and used for design purposes.

The following sections discuss each term in equation 12.1. Some common methods of estimation are presented that allow for practical use of the water-balance equation for design purposes. Other estimation methods also are often used throughout the world, some of which can be found in the references.

Precipitation, Air Temperature, and Solar Radiation

Precipitation and air temperature are the most common climatological data collected. Values of precipitation collected over at least a 20-year period at the location where the water balance is being calculated are the best data. If a short precipitation record (several years of daily values) is available on-site, and a longer record is available at a nearby site, interstation correlation of the on-site precipitation record with the longer-term record can be made. The result is a long-term synthetic precipitation record which is usually acceptable for design purposes. Figure 12.2 shows a typical interstation correlation for annual precipitation data.

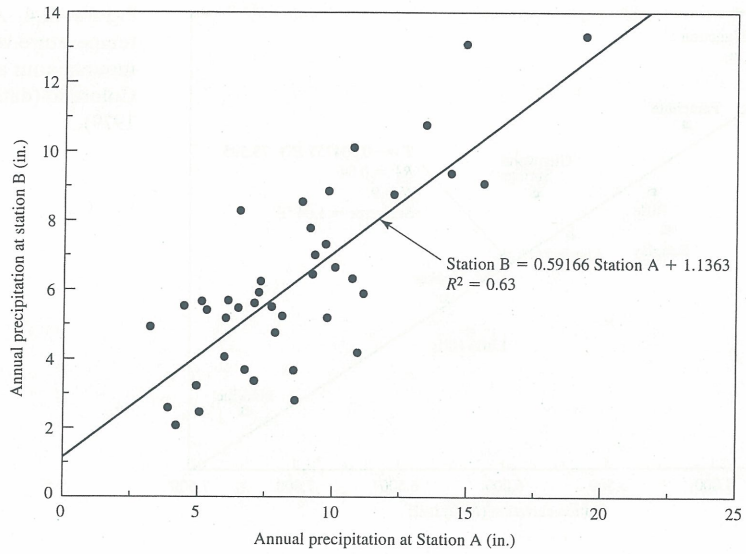

Figure 12.2 Interstation correlation of annual precipitation

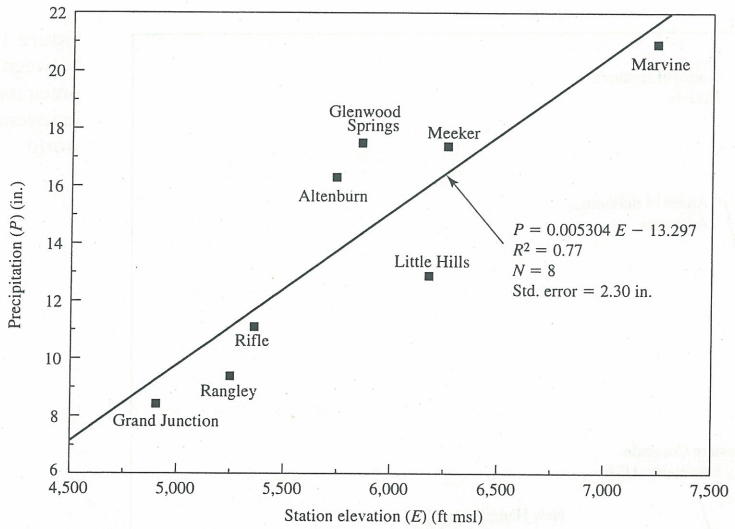

Figure 12.3 Average annual precipitation versus elevation for a mountainous area in Western Colorado (data from Wymore 1979)

If on-site precipitation data are unavailable, precipitation data (at a daily or longer time scale) may be "imported" from nearby stations. Transfer of precipitation (and air temperature) is possible if the data from the nearby station are adjusted for elevation and/or aspect prior to use at the site. Figures 12.3 and 12.4 show elevation adjustment of average annual precipitation and air temperature, respectively, for a mountainous area of western Colorado (Wymore 1979). Similar analyses can and should be made on a monthly basis. After obtaining the elevation adjustment from a long-term precipitation station to the site of interest, daily data can be imported using the adjustment variables applied to records for each day. Figure 12.5 shows relations between average annual precipitation and elevation in several regions of the world. It is important to note that a linear precipitation relation with elevation is not universal, and the relation may even be adverse—that is, precipitation may decrease with increasing elevation. Care is advised if large distances or large changes in elevation between stations are used; particular attention should be given to mountain ranges and large water bodies in the area of interest.

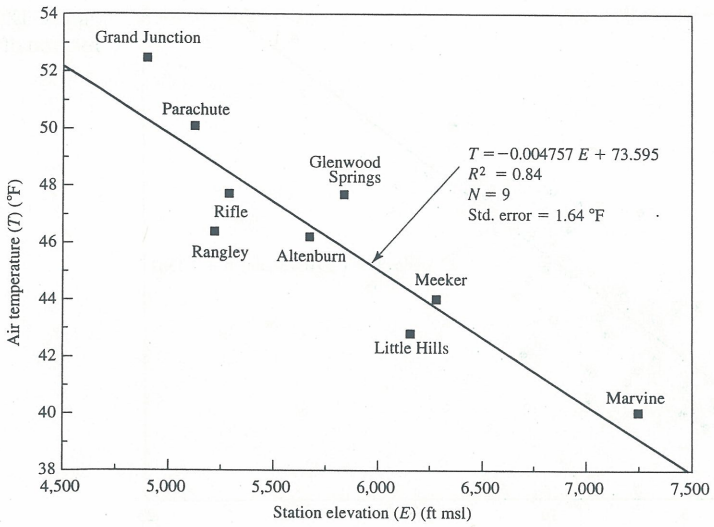

Figure 12.4 Average annual air temperature versus elevation for a mountainous area in Western Colorado (data from Wymore 1979)

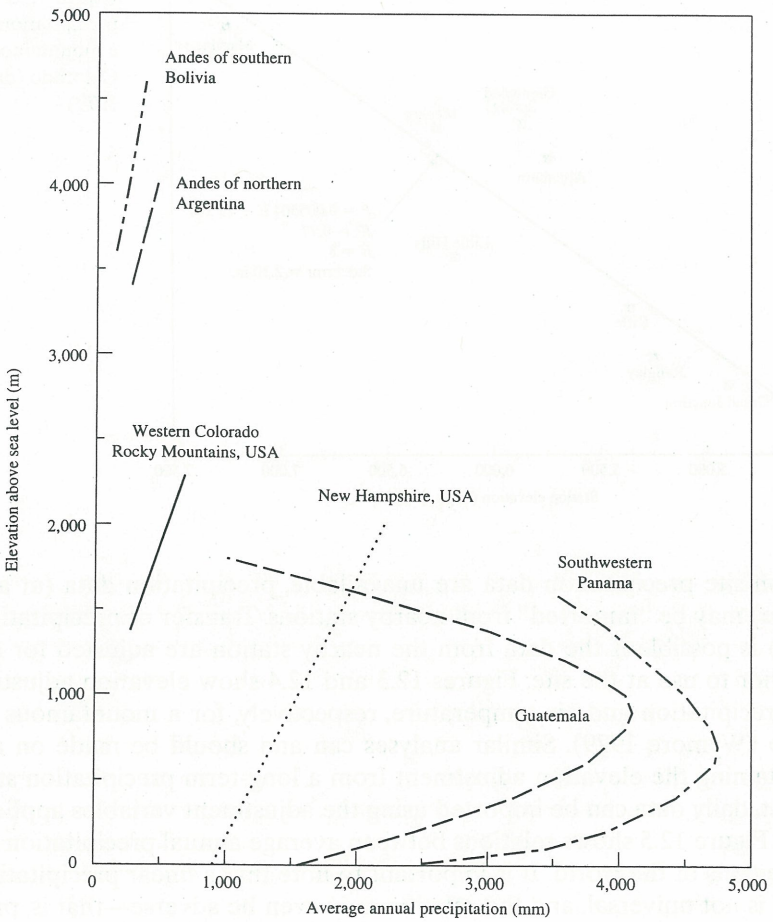

Figure 12.5 Relations between average annual precipitation and elevation in several regions of the world

If daily data are not available, they may be generated using a synthetic weather generator developed by the U.S. Agricultural Research Service (Richardson and Wright 1984). The most common source of this synthetic weather generator is the Hydrologic Evaluation of Landfill Performance (HELP) model (Schroeder et al. 1994a, b). Because daily precipitation and air temperature are usually available for many sites, the synthetic weather generator is most useful for calculating solar radiation, which often is not measured, is of poor quality, or is of short period of record.

Runoff

Runoff estimates for a water balance can be obtained from several possible sources. The best source is gaged-streamflow data in the drainage basin of interest. On-site or nearby gaged-streamflow data having a period-of-record of at least 20 years is ideal, but shorter records may be used. These gaged records can be extended using stochastic techniques (Fiering and Jackson 1971; Lane 1991; Lane and Frevert 1990; Grygier and Stedinger 1990; McLeod and Hipel 1978; Salas, Smith, and Markus 1992; Salas and Markus 1992). Both single-site and multisite runoff time series may be extended.

If sufficient runoff data are available in the basin, one method of transporting these data upstream or downstream is simply to adjust the runoff data for drainage-basin size or stream-channel length. Reliable estimates of runoff percentiles should include consideration that the flow rates can vary along a stream channel. In extreme cases, such as where a perennial stream discharges onto an alluvial fan, the losses can be sufficiently large to cause the stream to become ephemeral. Thus, care should be exercised in transporting data from one part of a drainage basin to another part of the same basin, using drainage area or channel length.

In hydrologically similar areas, a long-term gaged record can be correlated with another gaged record of shorter duration to obtain a predictive relation between the two records. Alternatively, multiple-regression methods can be used to develop a longer runoff record if some runoff records are available, along with those for longer-term climatological variables such as precipitation, air temperature, and pan evaporation. Multiple linear regression of runoff with the known variables provides a predictor for runoff. A typical regression-equation predictor is

$$Q = aB^eC^fD^g \tag{12.2}$$

where a, e, f, and g are regression constants, Q is runoff, and B, C, and D are hydrological and climatological variables of interest. Equation 12.2 is best-used to estimate annual values, but can be used with care to make seasonal estimates. A typical monthly rainfall-runoff correlation applying 32 months of data for a station in the Peruvian Andes—using only runoff and monthly precipitation—is shown in figure 12.6. The correlation in this case is fair, but might be improved by using air temperature and pan evaporation, in addition to precipitation, in the regression analysis.

Equation 12.2 can also be used to estimate runoff within a basin (or series of basins) where the hydrology is considered to be similar, but the variables B, C, and D are drainage-basin characteristics (e.g., basin area, channel slope, mean basin elevation, basin relief, basin perimeter), or other measurable basin variables that can be correlated with runoff. The multiple-correlation variables can also be a mixture of basin characteristics and climatological parameters. In the United States, the U.S. Geological Survey (USGS) and others have made studies of many drainage basins or regions using this technique. Examples can be found in Lowham (1976), Parker (1977), Craig and Rankl (1978), Masch (1984), and Christensen, Johnson, and Plantz 1986.

Where no runoff records are available for a stream, discharges for the time-period of interest are generated using climatological and drainage-basin data and information, such as

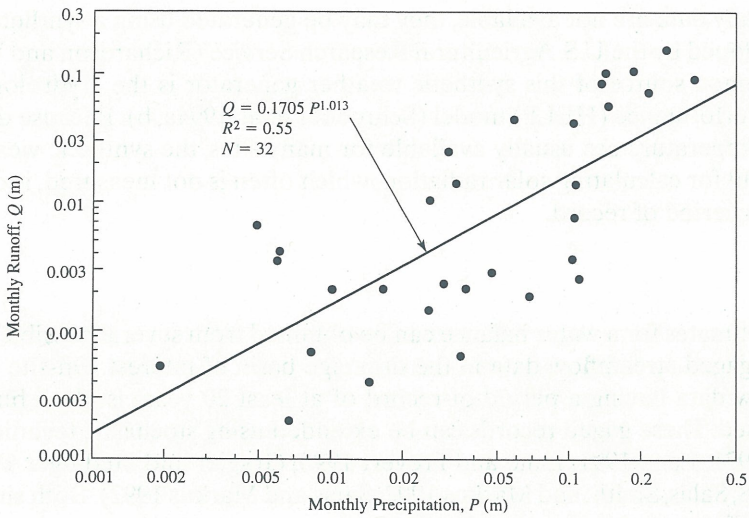

Figure 12.6 Typical rainfall/runoff relation, Peruvian Andes

precipitation, drainage-basin area and slope, basin soil and vegetation types, and general use. Many rainfall/runoff models, both simple and sophisticated, have been proposed to estimate runoff from climatological and drainage-basin data.

One of the easiest models to apply for estimating runoff from rainfall is the National Resources Conservation Service (NRCS) (formerly the SCS) model that was discussed in chapter 11, section 11.6. This model uses a curve number (CN) approach and is applicable to both specific storm events and to daily precipitation values (SCS 1985). The model uses precipitation, soil characteristics, and vegetative cover to develop runoff curve numbers.

Soil characteristics The SCS has classified over 5,000 soils into four hydrologic soil groups (Rawls, Brakensiek, and Saxton 1982). The definition of each soil group, along with limiting-infiltration rates by soil group, are given in chapter 11, table 11.2. The four hydrologic soil groups are designated as A, B, C, and D, in order of decreasing infiltration rate and increasing runoff potential. In general, soils in Group A are well-drained sands, whereas, soils in Group D are clay soils with high runoff potential (SCS 1985).

Vegetative-cover characteristics Some of the abstractions (losses) from precipitation falling on a basin are the result of vegetative cover. Additionally, vegetative cover or land use is an important factor not only in the volume, but in the rate of runoff as well. Generally, higher vegetative-cover densities result in lower runoff rates. Thus, curve numbers tend to be smaller for higher vegetative densities or for more pervious surfaces (SCS 1985).

Table 12.1 shows storm-event curve numbers based upon soil characteristics and vegetative cover for an average antecedent soil-moisture condition (SCS 1986). As shown in table 12.1, SCS runoff curve numbers have a wide range, depending upon the soil and vegetation characteristics; impervious surfaces and water surfaces are usually assigned curve numbers between 98 and 100. These curve numbers have not been well defined for areas of the world outside the United States; therefore, engineering judgment is necessary in order to select the correct curve number under different soil and vegetative characteristics overseas.

The curve numbers given in table 12.1 are for an average antecedent soil-moisture condition (AMC); the average condition is AMC II (SCS 1985). Recognizing that abstractions from precipitation depend upon the antecedent moisture condition existing at the time of the precipitation event, the SCS has defined three AMCs: AMC I is for conditions when little precipitation precedes an event, and the root-zone soils are relatively dry; AMC II is used when average antecedent precipitation has occurred prior to an event; and AMC III is used when considerable precipitation has occurred in the five days immediately prior to the precipitation

TABLE 12.1 Runoff Curve Number for Selected Land Uses (Antecedent Moisture Condition II)

Cover			Hydrologic soil group			
Land use or cover	Treatment or practice	Hydrologic condition	A	B	C	D
Fallow	Bare soil	—	77	86	91	94
	Crop residue[1]	Poor	76	85	90	93
		Good	74	83	88	90
Row Crops	Straight row	Poor	72	81	88	91
	Straight row	Good	67	78	85	89
	Contoured	Poor	70	79	84	88
	Contoured	Good	65	75	82	86
	Contoured and terraced	Poor	66	74	80	82
	Contoured and terraced	Good	62	71	78	81
Small grain	Straight row	Poor	65	76	84	88
	Straight row	Good	63	75	83	87
	Contoured	Poor	63	74	82	85
	Contoured	Good	61	73	81	84
	Contoured and terraced	Poor	61	72	79	82
	Contoured and terraced	Good	59	70	78	81
Close-seeded legumes or rotation meadow	Straight row	Poor	66	77	85	89
	Straight row	Good	58	72	81	85
	Contoured	Poor	64	75	83	85
	Contoured	Good	55	69	78	83
	Contoured and terraced	Poor	63	73	80	83
	Contoured and terraced	Good	51	67	76	80
Pasture or range[2]		Poor	68	79	86	89
		Fair	49	69	79	84
		Good	39	61	74	80
	Contoured	Poor	47	67	81	88
	Contoured	Fair	25	59	75	83
	Contoured	Good	6	35	70	79
Meadow		Good	30	58	71	78
Woods[3]		Poor	45	66	77	83
		Fair	36	60	73	79
		Good	30	55	70	77
Farmsteads		—	59	74	82	86
Roads	Dirt	—	72	82	87	89
	Hard surface	—	74	84	90	92
	Paved with curb and gutter	—	98	98	98	98
Commercial business areas	(85% impervious)	—	89	92	94	95
Industrial districts	(72% impervious)	—	81	88	91	93
Open spaces, lawns, parks, golf courses, cemeteries[4]		Poor	68	79	86	89
		Fair	49	69	79	84
		Fair	49	69	79	84
Residential lots	1/8 acre (65% impervious)		77	85	90	92
	1/4 acre (38% impervious)		61	75	83	87
	1/3 acre (30% impervious)		57	72	81	86
	1/2 acre (25% impervious)		54	70	80	85
	1 acre (20% impervious)		51	68	79	84
	2 acres (12% impervious)		46	65	77	82
Herbaceous[5]	Mixture of grass, weeds, and low growing brush, with brush the minor part	Poor		80	87	93
		Fair		71	81	89
		Good		62	74	85
Oak–Aspen[5]	Mountain brush mixture of oakbrush, aspen, mountain mahogany, bitter brush, maple, and other brush	Poor		66	74	79
		Fair		48	57	63
		Good		30	41	48

(*continued*)

TABLE 12.1 (*Continued*)

Land use or cover	Cover: Treatment or practice	Cover: Hydrologic condition	Hydrologic soil group: A	B	C	D
Piñon–Juniper[5]	Piñon, juniper or both with grass understory	Poor		75	85	89
		Fair		58	73	80
		Good		41	61	71
Sagebrush[5]	with grass understory	Poor		67	80	85
		Fair		51	63	70
		Good		35	47	55
Desert Shrub[5]	major plants include salt-bush, greasewood, creasotebush, blackbush, bursage, paloverde, mesquite and cactus	Poor	63	77	85	88
		Fair	55	72	81	86
		Good	49	68	79	84

Source: Data from SCS (1986)
[1]Applies only if residue is on at least 5% of surface throughout the year
[2]Poor: < 50% ground cover or heavily grazed with no mulch
Fair: 50% to 75% ground cover and not heavily grazed
Good: > 75% ground cover and lightly or only occasionally grazed
[3]Poor: Forest litter, small trees, and brush are destroyed by heavy grazing or regular burning
Fair: Woods are grazed but not burned, and some forest litter covers the soil
Good: Woods are protected from grazing, and litter and brush adequately cover the soil
[4]Poor: Grass cover < 50%
Fair: Grass cover 50% to 75%
Good: Grass cover > 75%
[5]Poor: < 30% ground cover (litter, grass, and brush overstory)
Fair: 30 to 70% ground cover
Good: > 70% ground cover

of interest. For most hydrologic designs, AMC II is used. Table 12.2 shows the AMC I and III curve-number values equivalent to those for AMC II.

The curve numbers are used to estimate runoff for a given depth of precipitation. Because the SCS curve numbers were originally developed for short-term storm events with rather high-intensity precipitation, they need to be adjusted if daily precipitation values are used. Schroeder et al. (1994a, b) use a correlation between minimum infiltration and soil type to calculate curve numbers for use with daily precipitation values. These curve numbers are shown for various soil textures and vegetation covers in figure 12.7. Both the Unified Soil Classification System (USCS) and the U.S. Department of Agriculture (USDA) soil-classification systems are shown in figure 12.7. The curve numbers shown in figure 12.7 are similar to those shown in the HELP model (Schroeder et al. 1994a, b), but can vary slightly for fair, good, and excellent grass covers. The definitions of both USDA and USCS soil classifications are given in table 12.3; the USDA soil textures shown in table 12.3 can be converted to USCS classifications using a soil-classification triangle provided by McAneny et al. 1985.

QUESTION 12.1

Extension of climatological records using interstation correlation is a common method used to augment data at a site having a short period of record. In the answer to this question at the end of the chapter, pan evaporation data for four climatological stations are tabulated. Stations A and B have 24 and 27 years, respectively, of pan evaporation data. Station C has 13 years of data. The objective is to extend the pan evaporation record of Station Z using interstation correlations with the other three climatological stations. Try several methods, including multiple linear and nonlinear regression.

TABLE 12.2 Equivalent Curve Numbers for AMC I and AMC III Conditions Given AMC II Curve Number

CN for AMC II	CN for AMC Conditions		CN for AMC II	CN for AMC Conditions	
	I	III		I	III
100	100	100	60	40	78
99	97	100	59	39	77
98	98	99	58	38	76
97	91	99	57	37	75
96	89	99	56	36	75
95	87	98	55	35	74
94	85	98	54	34	73
93	83	98	53	33	72
92	81	97	52	32	71
91	80	97	51	31	70
90	78	96	50	31	70
89	76	96	49	30	69
88	75	95	48	29	68
87	73	95	47	28	67
86	72	94	46	27	66
85	70	94	45	26	65
84	68	93	44	25	64
83	67	93	43	25	63
82	66	92	42	24	62
81	64	92	41	23	61
80	63	91	40	22	60
79	62	91	39	21	59
78	60	90	38	21	58
77	59	89	37	20	57
76	58	89	36	19	56
75	57	88	35	18	55
74	55	88	34	18	54
73	54	87	33	17	53
72	53	86	32	16	52
71	52	86	31	16	51
70	51	85	30	15	50
69	50	84	25	12	43
68	48	84			
67	47	83	20	9	37
66	46	82	15	6	30
65	45	82			
64	44	81	10	4	22
63	43	80	5	2	13
62	42	79	0	0	0
61	41	78			

Source: Data from SCS, 1985.

Snowmelt Prediction of snowmelt runoff generally uses one of two approaches: the energy-balance approach and the temperature-index approach. The physically based energy-balance approach uses a multiple-phase technique (solid and liquid water) of bringing the snowpack from a temperature less than the freezing point of water to 0 °C, ripening the snowpack and finally, computing the melt on a time-dependent basis. The time period used in many energy-balance snowmelt models is hourly. Clearly, the energy-balance snowmelt approach requires measurement of many climatological and snowpack variables; these include: air temperature, relative humidity, wind speed, cloud cover or solar radiation, precipitation,

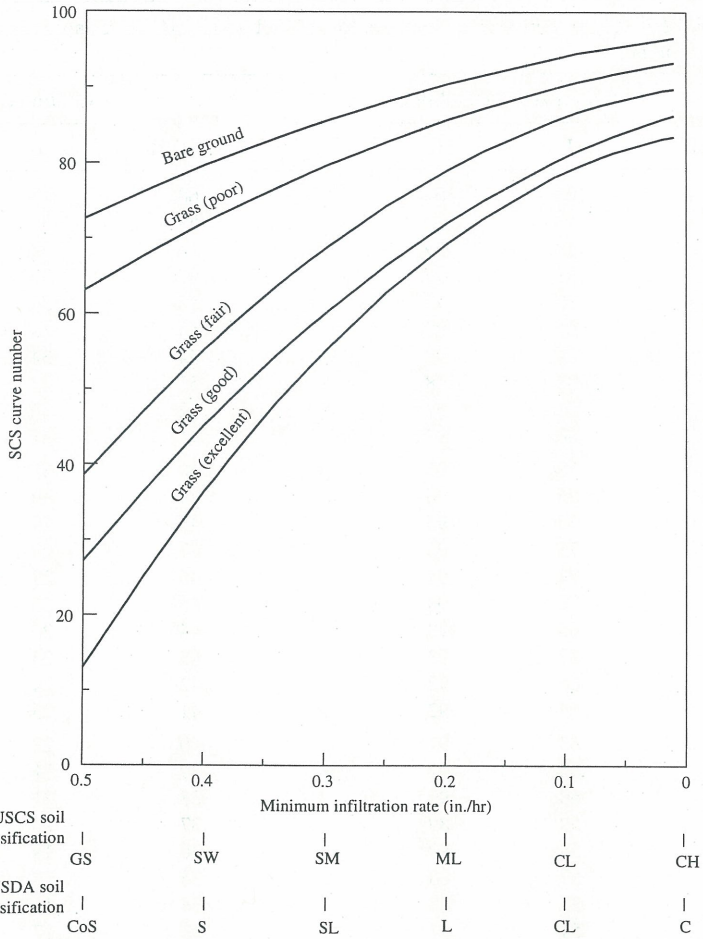

Figure 12.7 Relation between SCS curve number for daily precipitation and soil texture for various vegetative covers (data from Schroeder et al. 1994b)

TABLE 12.3 Definition of USCS and USDA Soil-Texture Classifications

USCS	Definition	USDA	Definition
G	Gravel	G	Gravel
S	Sand	S	Sand
M	Silt	Si	Silt
C	Clay	C	Clay
P	Poorly graded	L	Loam (sand, silt, clay, and humus mixture)
W	Well-graded	Co	Coarse
H	High plasticity or compressibility	F	Fine
L	Low plasticity or compressibility		

Source: Data from Schroeder et al. 1994b.

snow temperature, snow density, and initial snow water content. These data need to be available hourly, or at a minimum, as daily averages. Therefore, the energy-balance approach is often data-limited, especially in remote areas. More details on this approach can be found in U.S. Army Corps of Engineers (USACOE, 1956), Dingman (1994), Rantz (1964), Federer (1968), Anderson (1968; 1976), and are not included in detail here.

The temperature-index approach is the easiest and most common method used to estimate snowmelt, especially in areas where detailed climatological data are limited or not

TABLE 12.4 Selected Equations for Snowmelt Coefficient[1]

Equation	Reference
$A = 0.4 f_S\,(1 - a)e^{-4F}$	Male and Gray (1981)
$A = f_F\,(0.7 + 0.0099\mathrm{J})f_S, J < 183$	Federer and Lash (1978)
$A = 0.07\,(1 + F) + [0.029 + (1 - 0.7F)(0.0084w) + 0.007Pr]$	Rantz (1964)
$A = 0.00629\,(z_a z_b)^{-1/6}(P/P_o)w$	Corps of Engineers (1956)

[1]Values for A in the equation $Q = A(T_a - T_m)$.

Notes:

A = melt coefficient in cm °C^{-1} day^{-1} for Male and Gray (1981); in inches °F^{-1} day^{-1} for Federer and Lash; Rantz; and Corps of Engineers
a = albedo
F = fraction of forest cover in Male and Gray (1981); forest density as a decimal in Rantz
f_S = ratio of solar radiation received at the site of interest to that on a horizontal surface
f_F = vegetative factor equal to 3.0 for open areas, 1.75 for hardwood forests, and 1.0 for conifer forests
J = Julian day
Pr = daily rainfall in inches
P = vapor pressure in mb
P_o = saturation vapor pressure at T_a in mb
T_a = average air temperature in °C in Male and Gray (1981), °F in the other equations
T_m = average snow surface temperature in °C in Male and Gray (1981), °F in the other equations
w = mean wind velocity in mph at 50 feet above ground in Rantz; mean wind velocity near surface of ground in mph for Corps of Engineers
z_a = height above ground, where T_a and P are measured in feet
z_b = height above ground, where w is measured in feet

available. The approach was popularized by the USACOE (1956), later detailed by Federer and Lash (1978) and Gray and Prowse (1993). Snowmelt for a typical daily time period, using the temperature-index approach, is a linear function of average air temperature given as

$$Q = A(T_a - T_m) \tag{12.3}$$

where Q is snowmelt in equivalent depth of water, T_a is air temperature, and T_m is snow melting-point temperature (usually taken as 0 °C), and A is a melt coefficient. The melt coefficient, A, is not a simple constant but includes such variables as latitude, elevation, basin slope and aspect, and type of forest cover. Therefore, A should be developed from data empirically; many empirical equations have been proposed for the snowmelt coefficient. Table 12.4 presents some of these snowmelt-coefficient equations and their units.

Evaporation/Transpiration

Free-water surface and wet-soil surface evaporation Pan-evaporation data are a good estimate of free-water surface and wet-soil surface evaporation. Because year-to-year variations in evaporation are usually small, a few years of data (typically three or more) provide a satisfactory estimate of annual and even monthly values. A good source of evaporation data in the United States is the Climatic Atlas (Environmental Science Service Administration (ESSA) 1983). In other countries, local climatological data often include pan- or lake-evaporation data.

Free-water surface evaporation can be calculated, in the absence of measured data, using a form of Dalton's (1802) law

$$E = C(e_w - e_a) \tag{12.4}$$

where E is evaporation rate, C is an empirical coefficient, e_w is maximum (saturation) vapor pressure, and e_a is actual vapor pressure. The vapor-pressure gradient, $e_w - e_a$, is the driving force for free-water surface and wet-soil surface evaporation. Several factors can affect either the vapor-pressure gradient or the empirical coefficient in equation 12.4; these factors

include: air and water temperature, wind over the wet surface, atmospheric pressure, soluble solids in the water evaporating, and the nature and shape of the water surface.

Temperature generally increases the vapor-pressure gradient and therefore, evaporation rates. Increased evaporation is caused either by increasing the temperature of the water body, or by increasing the temperature of the air so that more water can be stored in the air without causing vapor saturation. Wind velocities over the wet surface also tend to increase the evaporation rates by keeping the air at less-than saturation.

Decreased atmospheric pressures, usually caused by increases in elevation, can cause increased vapor-pressure gradients that result in increased free-water surface evaporation. Increases in dissolved solids in the water decrease the vapor-pressure gradient, thus decreasing evaporation. The shape of the water surface also influences the quantity of free-water surface evaporation; a flat-water surface has a greater vapor-pressure gradient than a concave-upward surface. Also, evaporation through small surface openings such as tanks, is proportional to the diameter or perimeter of the opening, rather than its surface area.

Table 12.5 summarizes some of the commonly used free-water surface evaporation equations, physically based upon Dalton's law. These equations have the basic form of equa-

TABLE 12.5 Free Water-Surface Evaporation Equations Based upon Dalton's Law

Equation	Reference
$E = C\,(e_w - e_a)$	Dalton (1802)
$E = \psi(e_w - e_a)$, where $\psi = 0.4 + 0.199\,w$	FitzGerald (1886)
$E = C(e_w - e_a)\,\psi$, where $\psi = 1 + 0.1w$	Meyer (1915)
$E = 0.4(\psi e_w - e_a)$, where $\psi = 2 - e^{-0.2w}$	
For large areas, E is multiplied by $(I - P) + P\dfrac{\psi - 1}{\psi - h}$	Horton (1917)
$E = 0.771(1.465 - 0.186B)\,\psi\,(e_w - e_a)$, where $\psi = 0.44 + 0.188w$	Rohwer (1931)
$E = 0.00177w(e_w - e_a)$	Harbeck and others (1954)
$E = 0.001813w(e_w - e_a)t[1 - 0.03(T_a - T_w)]$	Harbeck and others (1958)
$E = 0.7[E_{pan} \pm 0.00064P_a\alpha(0.37 + 0.00255w)\lvert T_{wpan} - T_a\rvert^{0.36}]$ when $T_{wpan} > T_a$, sign is +; when $T_{wpan} < T_a$, sign is −	Kohler and others (1955)
$E = [0.0211 + (9.24 \times 10^{-4})(T_w - T_a) + (1.19 \times 10^{-4})w](e_w - e_a)$	Dingman and others (1968)

Notes:

B = mean barometric reading in inches of Hg at 32 °F

C = coefficient depending upon various uncounted factors affecting evaporation; or $C = 15$ for small, shallow water and $C = 11$ for large, deep water in monthly Meyer equation, $C = 0.5$ and 0.37 for daily Meyer equation

e_a = actual vapor pressure in air based upon monthly mean air temperature and relative humidity at 30 ft above water surface in Meyer equation; mean pressure at water-surface temperature in mb in Harbeck and Dingman equations; inches of Hg in other equations

e_w = maximum (saturation) vapor pressure in inches of Hg based upon monthly mean air temperature corresponding to water temperature in Meyer equation; mean vapor pressure at water-surface temperature in mb in Harbeck and Dingman equations; inches of Hg in other equations

E = evaporation rate in inches per 30-day month or daily in Meyer equation; in inches per t days in Harbeck equation; cm per day in Dingman and Kohler equations; inches per day in other equations

E_{pan} = measured pan evaporation in cm per day

h = relative humidity

P = percentage of time during which wind is turbulent

P_a = atmospheric pressure in mb

t = number of days in period for evaporation

T_a = average air temperature, °C + 1.9 °C in Harbeck equation; °C in other equations

T_w = average water surface temperature in °C

T_{wpan} = evaporation pan water-surface temperature in °C

w = monthly wind velocity in mph at 30 ft above ground in Meyer equation; mean wind velocity near surface of ground in knots for Harbeck (1958) equation; average wind velocity at 15 cm above pan for Kohler equation; average wind velocity near surface of ground in kilometers per day for Dingman equation; mph in other equations

α = proportion of energy lost from the evaporation pan in the Kohler equation, $\alpha = 0.34 + 0.0117T_w - (3.5 \times 10^{-7})(T_w + 17.8)^3 + 0.0135w^{0.36}$

ψ = wind factor

tion 12.4, with terms for increasing or decreasing the evaporation based upon the factors discussed above.

Monthly evaporation: Meyer equation Data from Viehmeyer and Brooks (1954) indicate that evaporation from a wet-soil surface (where the soil is near saturation) is approximately the same as that from a free-water surface. Thus, the Meyer equation—or some similar equation based upon Dalton's law—is a good approximation of evaporation from both a free-water surface and a wet-soil surface. Other free-water surface-evaporation equations shown in table 12.5 can also be used if sufficient data are available. The Meyer equation is described as

$$E = C(e_w - e_a)\psi, \qquad \psi = 1 + 0.1w \tag{12.5}$$

In the Meyer equation applied monthly, $C = 15$ for small, shallow-water bodies and $C = 11$ for large, deep-water bodies. The maximum and actual vapor pressures e_w and e_a, respectively, are in inches of mercury (Hg), corresponding to the monthly mean-air temperature and relative humidity. The wind factor, ψ, is calculated from the monthly mean-wind velocity, w, in miles per hour (mph) at a height of 30 feet (10 meters) above the water or wet-soil surface.

The maximum vapor pressure (saturation-vapor pressure) over water is given by

$$e_w = (0.0041T + 0.676)^8 - 0.000019|T + 16| + 0.001316 \tag{12.6}$$

where $-60\ °\text{F} \leq T \leq 130\ °\text{F}$ and e_w is in inches of Hg. The actual vapor pressure is given by the definition of relative humidity rH and

$$\text{rH} = \frac{e_a}{e_w} \tag{12.7}$$

or

$$e_a = e_w \text{rH} \tag{12.8}$$

The Meyer equation can also be used daily if the coefficient C is divided by 30 days and the temperature, wind velocity, and relative humidity are all daily mean values. In this case, the values of $C = 0.50$ for small, shallow-water bodies and $C = 0.37$ for large, deep-water bodies.

Evapotranspiration Evapotranspiration is composed of four components: **(1)** evaporation from the wet soil near the vegetation; **(2)** transpiration of water by the vegetation; **(3)** evaporation from the moist membrane surfaces of the vegetation; and **(4)** use of water by the vegetation to build new plant tissue (Blaney and Hanson 1965). Evapotranspiration is the same as consumptive use, a term often used by water-rights engineers.

Several factors affect evapotranspiration, among them air temperature, wind speed, solar radiation, and available soil moisture. As indicated by Dalton's law (equation 12.4), the driving force for evaporation as well as evapotranspiration is vapor-pressure gradient, itself highly dependent upon air temperature; the vapor-pressure gradient and resulting evapotranspiration increase with increasing air temperature. Wind speed also affects evapotranspiration by removing water vapor immediately above wet soil and plant membranes; therefore, increased wind speed results in increased evapotranspiration. The primary source of evapotranspiration energy is solar radiation; increased solar radiation results in increased evapotranspiration.

Even though the above climatological factors can act to increase evapotranspiration, vegetation only transpires if sufficient soil moisture is available. If soil-water contents are limiting, evapotranspiration is limited by the ability of the vegetation to extract water from the soil. Additionally, plant factors are important in transpiration. Research on revegetation of retorted-oil shale in Colorado (Berg et al. 1979; Herron, Berg, and Harbert 1980; Kilkelly 1981; Jump and Sabey 1983) has shown that during times of water stress, natural vegetation transpires less water, reduces growth, sheds leaves, and closes their stomata to conserve water. Thus, plant factors can be important in controlling evapotranspiration in arid and

semiarid areas. In general, increased soil water results in increased—or at least does not limit—evapotranspiration. Soil moisture has to be above wilting point for evapotranspiration to occur at the rate predicted by the theoretical equations.

There are three common methods for estimating evapotranspiration: **(1)** temperature methods; **(2)** radiation methods; and **(3)** combination of temperature and radiation methods (Jensen, Burman, and Allen 1990). It has been shown that combination methods provide the best models for estimating evapotranspiration. All estimation methods predict potential evapotranspiration (PET) for a reference crop (such as short grass or alfalfa). Actual evapotranspiration for a given type of vegetative cover or crop is estimated by multiplying PET by an appropriate crop coefficient. Vegetative or crop coefficients are both annual and seasonal, and can be obtained from various sources in the literature. Often these coefficients are site-dependent, so care needs to be taken to assure that the vegetative coefficients in use were determined for conditions similar to those occurring at the site of interest; coefficients for selected vegetation are given below.

Temperature method: Blaney–Criddle The generally recommended temperature method for estimating monthly evapotranspiration is the Blaney–Criddle method (Blaney and Criddle 1950; 1957; 1962). The original method was developed for estimation of evapotranspiration seasonally (growing season). The assumption is that evapotranspiration varies directly with the sum of the products of mean-monthly air temperature and monthly percentage of daytime hours, for an actively growing crop with adequate soil moisture. This relation is given mathematically by

$$U = KF = \sum_{i=1}^{m} u_m = \sum_{i=1}^{m} k_c k_t f \tag{12.9}$$

where U is the seasonal evapotranspiration (consumptive use) in inches for the growing season of interest; K is an empirical consumptive-use coefficient (growing season/growing period); F is the sum of monthly consumptive-use factors; f, for the season or period; u_m is the monthly consumptive use in inches; k_c is the monthly empirical-crop coefficient; and k_t is the monthly temperature coefficient. The monthly temperature coefficient is given by

$$k_t = 0.0173t - 0.314 \tag{12.10}$$

where t is the monthly mean-air temperature in °F. The monthly consumptive-use factor is given by

$$f = \frac{tp}{100} \tag{12.11}$$

where p is monthly percentage of daytime hours of the year. Individual monthly evapotranspiration is given by $u_m = k_c k_t f$ for the month of interest. Table 12.6 presents monthly percentages of daytime hours by latitude (SCS 1970). Monthly and annual empirical-crop coefficients for various crops and natural vegetation are shown on table 12.7. SCS (1970) presents curves of crop coefficients for use with the Blaney–Criddle method; Pochop, Borrell, and Burman (1984) recommend an elevation-correction for the Blaney–Criddle equation that increases the evapotranspiration by approximately 10 percent for each 1,000-meter increase in elevation. This correction adjusts for lower temperatures that occur at higher elevations, at a given level of solar radiation.

Doorenbos and Pruitt (1977) modified the Blaney–Criddle method to compute evapotranspiration for a grass-related reference crop. The FAO-24 Blaney–Criddle method requires the intermediate step of estimating a grass-related reference crop evapotranspiration, E_{to}, prior to applying grass-related crop coefficients.

Radiation method: Jensen–Haise The Jensen–Haise method (Jensen and Haise 1963) is recommended for estimating evapotranspiration every five days, but can also be used to

TABLE 12.6 Monthly Percentage of Daytime Hours, p, of the Year

Latitude (deg.)	Jan.	Feb.	March	April	May	June	July	Aug.	Sept.	Oct.	Nov.	Dec.
						North						
60	4.70	5.67	8.11	9.69	11.78	12.41	12.31	10.68	8.54	6.95	5.02	4.14
55	5.44	6.04	8.18	9.44	11.15	11.53	11.54	10.29	8.51	7.23	5.63	5.02
50	5.99	6.32	8.24	9.24	10.68	10.92	10.99	9.99	8.46	7.44	6.08	5.65
45	6.40	6.54	8.29	9.08	10.31	10.46	10.57	9.75	8.42	7.61	6.43	6.14
40	6.75	6.72	8.32	8.93	10.01	10.09	10.22	9.55	8.39	7.75	6.73	6.54
35	7.04	6.88	8.35	8.82	9.76	9.76	9.93	9.37	8.36	7.88	6.98	6.87
30	7.31	7.02	8.37	8.71	9.54	9.49	9.67	9.21	8.33	7.99	7.20	7.16
25	7.54	7.14	8.39	8.62	9.33	9.24	9.45	9.08	8.31	8.08	7.40	7.42
20	7.75	7.26	8.41	8.53	9.15	9.02	9.24	8.95	8.29	8.17	7.58	7.65
15	7.94	7.37	8.43	8.45	8.98	8.81	9.04	8.83	8.27	8.25	7.75	7.89
10	8.14	7.47	8.45	8.37	8.81	8.61	8.85	8.71	8.25	8.34	7.91	8.09
5	8.32	7.67	8.47	8.29	8.85	8.41	8.67	8.60	8.24	8.41	8.07	8.30
0	8.50	7.67	8.49	8.22	8.49	8.22	8.50	8.49	8.21	8.49	8.22	8.50
						South						
10	8.86	7.87	8.53	8.09	8.18	7.86	8.14	8.27	8.17	8.62	8.53	8.88
20	9.24	8.09	8.57	7.94	7.85	7.43	7.76	8.03	8.13	8.76	8.87	9.33
30	9.70	8.33	8.62	7.73	7.45	6.96	7.31	7.76	8.07	8.97	9.24	9.85
40	10.27	8.63	8.67	7.49	6.97	6.37	6.76	7.41	8.02	9.21	9.71	10.49

Source: Data from SCS, 1970

TABLE 12.7 Typical Seasonal Blaney–Criddle Growth-Stage Coefficients (k_c)

	Growth-Stage Coefficient												
Crop	Jan.	Feb.	March	April	May	June	July	Aug.	Sept.	Oct.	Nov.	Dec.	Annual[1]
Alfalfa	0.63	0.73	0.86	0.99	1.08	1.13	1.11	1.06	0.99	0.91	0.78	0.64	0.80–0.90
Pasture Grasse	0.49	0.57	0.73	0.86	0.90	0.92	0.92	0.91	0.87	0.79	0.67	0.55	0.75–0.85
Greasewood[2]	0.50	0.58	0.63	0.85	0.99	1.56	2.00	2.40	2.50	2.10	1.49	0.85	—
Greasewood[3]	0.35	0.39	0.40	0.45	0.52	0.84	1.10	1.29	1.35	1.12	0.80	0.45	—
Greasewood[4]	0.15	0.16	0.18	0.19	0.20	0.34	0.44	0.52	0.55	0.45	0.32	0.19	—
Saltcedar	—	—	—	—	—	—	—	—	—	—	—	—	1.40–1.50
Cottonwood	—	—	—	—	—	—	—	—	—	—	—	—	1.15–1.25
Phreatophytic Bushes	—	—	—	—	—	—	—	—	—	—	—	—	0.90–1.00
Bermuda grass (high values)	1.17	1.07	1.27	1.28	1.22	0.81	0.68	0.73	0.74	1.03	0.95	0.72	—
Bermuda grass (low values)	—	0.44	0.42	0.83	0.81	0.76	0.58	0.53	0.58	0.77	1.02	0.44	—

Sources: Data from Blaney and Hanson, 1965; SCS, 1970; Pochop and others, 1984

[1]Values of K. Lower values are for humid areas and higher values are for arid climates.

[2]0–12 in. of water

[3]18–36 in. of water

[4]36–60 in. of water

estimate evapotranspiration daily, if care is used. The Jensen–Haise method uses the equation

$$E_{tp} = C_t(T - T_x)R_s \tag{12.12}$$

where E_{tp} is daily evapotranspiration in inches, C_t is the temperature coefficient, T is mean-air temperature in °F, T_x is the temperature-scale intercept when $ET/R_s = 0$, and R_s is solar radiation in inches/day of evaporation.

Also,

$$C_t = \frac{1}{C_1 + C_2C_h} \tag{12.13}$$

and

$$C_h = \frac{50\,mb}{e_2 - e_1} \tag{12.14}$$

where e_1 and e_2 are saturated vapor pressures at the mean-maximum and -minimum air temperatures for the warmest months of the year; and

$$C_2 = 13\ ^\circ\text{F} \tag{12.15}$$

Also,

$$C_1 = 68 - \frac{3.6E}{1000} \tag{12.16}$$

where E = site elevation in feet, and

$$T_x = 27.5 - 0.25(e_2 - e_1) - \frac{E}{1000} \tag{12.17}$$

If daily solar radiation data are not available, they can be calculated using either stochastic techniques (Richardson and Wright 1984; Schroeder et al. 1994a, b), or from cloudless-sky radiation (see table 12.8), using

$$R_s = R_{so}\left[1 - (1 - k)\frac{n}{10}\right] \tag{12.18}$$

TABLE 12.8 Mean Solar Radiation for Cloudless Skies

	Mean solar radiation per month (cal/cm²/day)*											
Latitude	Jan.	Feb.	March	April	May	June	July	Aug.	Sept.	Oct.	Nov.	Dec.
60 N	58	152	319	533	671	763	690	539	377	197	87	35
55 N	100	219	377	558	690	780	706	577	430	252	133	74
50 N	155	290	429	617	716	790	729	616	480	313	193	126
45 N	216	365	477	650	729	797	748	648	527	371	260	190
40 N	284	432	529	677	742	800	755	674	567	426	323	248
35 N	345	496	568	700	742	800	761	697	603	474	380	313
30 N	403	549	600	713	742	793	755	703	637	519	437	371
25 N	455	595	629	720	742	780	745	703	660	561	486	423
20 N	500	634	652	720	726	760	729	697	680	597	537	474
15 N	545	673	671	713	706	733	706	684	697	623	580	519
10 N	584	701	681	707	684	700	681	665	707	648	617	565
5 N	623	722	690	700	652	663	645	645	710	665	650	606
0 N	652	740	694	680	623	627	616	623	707	684	680	619
5 S	648	758	690	663	590	587	577	590	693	690	727	677
10 S	710	772	681	640	571	543	526	558	680	690	727	710
15 S	729	779	665	610	516	497	497	519	657	687	747	739
20 S	748	779	645	573	474	447	445	481	630	677	753	761
25 S	761	779	626	533	419	400	406	439	600	665	767	777
30 S	771	772	600	497	384	353	358	390	567	648	767	793
35 S	774	754	568	453	335	300	310	342	530	629	767	806
40 S	774	729	529	407	281	243	261	290	477	603	760	813
45 S	774	704	490	357	229	183	203	235	447	571	747	813
50 S	761	669	445	307	174	127	148	177	400	535	727	806
55 S	748	630	397	250	123	77	97	123	343	497	707	794
60 S	729	588	348	187	77	33	52	74	283	455	700	787

Source: Data from Budyko 1963

*1 cal/cm²/day = 1004.515 kilowatts/m²

where R_s is solar radiation at the ground surface in langleys per day (cal cm^{-2} d^{-1}), R_{so} is cloudless-sky radiation in langleys per day, k is a mean-annual coefficient (see table 12.9), and n is cloudcover in tenths ($0 \leq n \leq 10$). Note that, to convert radiation from langleys per day (cal cm^{-2} d^{-1}) to inches per day, multiply by 0.000673; and to convert langleys per day to kilowatts per square meter (kW/m^2), multiply by 0.000484.

Crop coefficients for the Jensen–Haise method have been published by Jensen et al. (1971; 1990). Generalized Jensen–Haise crop coefficient for various crops, including alfalfa and pasture grass, are presented in figures 12.8 through 12.11. These generalized coefficients can also be used with the FAO–Penman method (presented following), or other PET methods.

Combination method: FAO–Penman This method (Doorenbos and Pruitt 1977) is recommended for estimating daily evapotranspiration. Details on the use of this method—as well as comparison of the results of this method to other evapotranspiration methods—are presented in Jensen, Burman, and Allen (1990), and were discussed in chapter 9. The basic equation for the FAO–Penman method is

$$E_o = c\left[\frac{\Delta}{\Delta + \gamma}(R_n - G) + \frac{\gamma}{\Delta + \gamma} 2.7 W_f (e_z^w - e_z)\right] \tag{12.19}$$

where E_o is the evapotranspiration for a grass-reference crop, c is an adjustment factor based on local climate, and W_f is wind factor given by $(1 + 0.864\, u_2)$; the other variables are defined below. In equation 12.19, E_o and R_n are in mm/day, u_2 is in m/s, and e is in kPa; G is assumed to be zero for daily periods in the FAO–Penman method. The vapor-pressure deficit is

TABLE 12.9 Mean Annual Values of k for Use in Converting Cloudless Sky Radiation to Actual Solar Radiation

Latitude (degrees North or South)												
0	5	10	15	20	25	30	35	40	45	50	55	60
0.35	0.34	0.34	0.33	0.33	0.32	0.32	0.32	0.33	0.34	0.36	0.38	0.40

Source: Data from Jensen, Burman, and Allen 1990

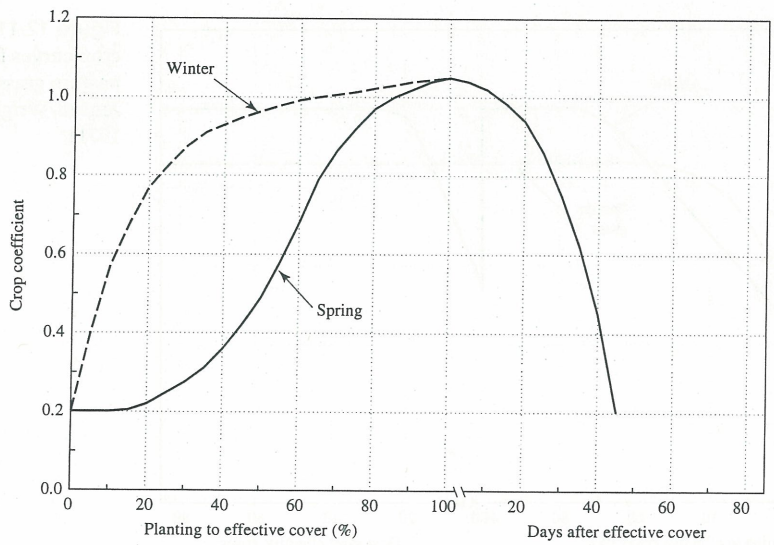

Figure 12.8 Jensen–Haise crop curves for small grains (data from Jensen, Wright, and Pratt 1971)

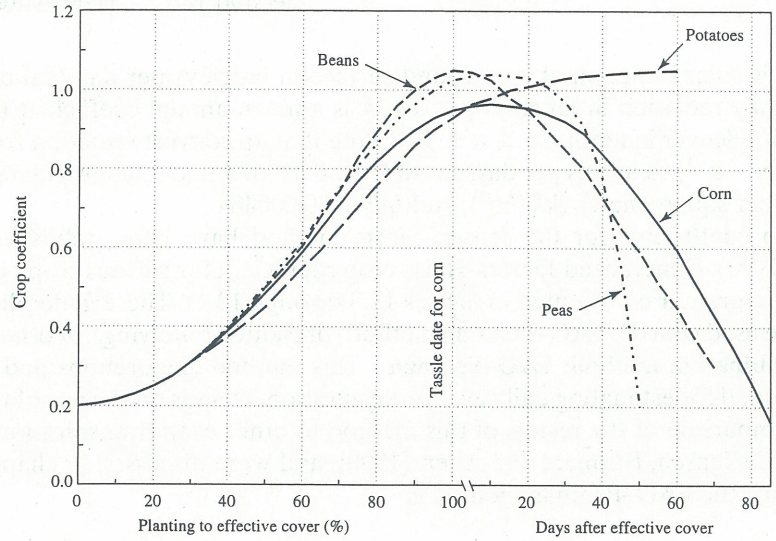

Figure 12.9 Jensen–Haise crop curves for beans, potatoes, peas, and corn (data from Jensen, Wright, and Pratt 1971)

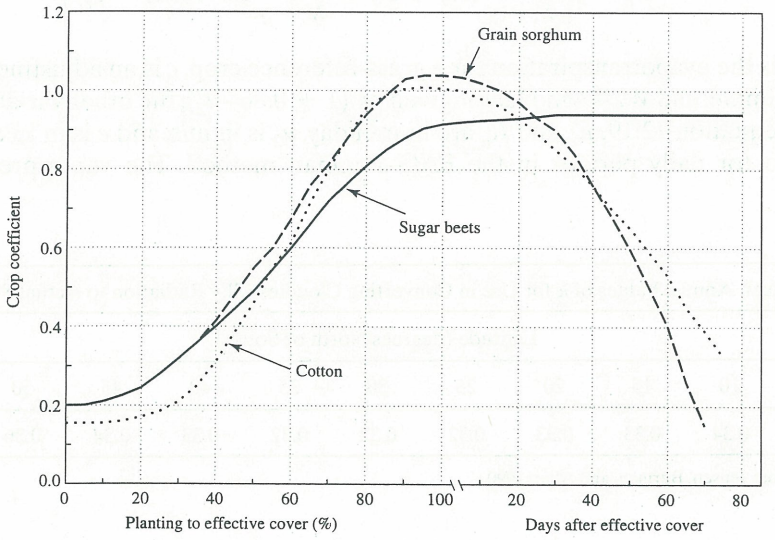

Figure 12.10 Jensen–Haise crop curves for sugar beets, grain sorghum, and cotton (data from Jensen, Wright, and Pratt 1971)

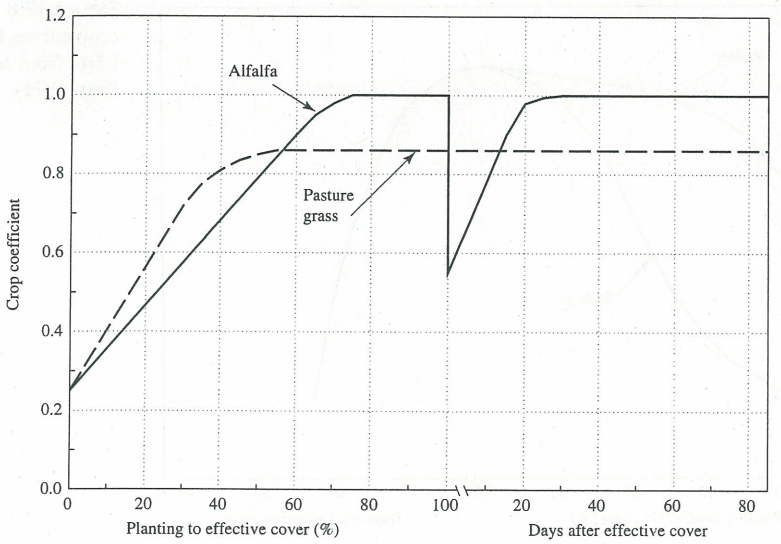

Figure 12.11 Jensen–Haise crop curves for alfalfa and pasture grass (data from Jensen, Wright, and Pratt 1971)

calculated by Method 1 (equation 12.20) when dewpoint-temperature data are available, otherwise Method 2 (equation 12.21) is used:

Method 1

$$(e_z^w - e_z) = e_w(T_{\text{mean}}) - e_w(T_{\text{dew}}) \tag{12.20}$$

Method 2

$$(e_z^w - e_z) = e_w(T_{\text{mean}})(1 - \text{rH}/100) \tag{12.21}$$

The adjustment factor c is given by

$$c = 0.68 + 0.0028\,\text{rH}_{\max} + 0.018\,R_s - 0.068U_d + 0.013U_d/U_n + 0.0097U_d(U_d/U_n) + 0.430 \times 10^{-4}\,\text{rH}_{\max}R_sU_d \tag{12.22}$$

where $\text{rH}_{\max}$ is maximum daily relative humidity in percentage; R_s is in mm/day; U_d/U_n is the ratio of the daytime to nighttime wind speed; U_d is the daytime (0700–1900 hrs) windspeed in m s^{-1}; R_n is net-solar radiation; R_s is incident-solar radiation; G is soil-heat flux (assumed to be zero for daily time periods); and Δ is the slope of the saturation vapor pressure versus air temperature curve, and is given by

$$\Delta = \frac{de_w}{dT} = 0.200(0.00738\,T + 0.8072)^7 - 0.000116 \tag{12.23}$$

for $T \geq -23$ °C and Δ = kPa/°C. The psychrometric constant γ is given by

$$\gamma = \frac{c_pP}{0.622L_v} \tag{12.24}$$

where the units are in kPa/°C, and P is atmospheric pressure in kPa, c_p is the specific heat of moist air at a constant pressure of 1.013 kJ/kg − °C, and L_v is the latent heat of vaporization of water, in kJ/kg.

Pan-evaporation method Often, pan-evaporation data are available. Estimates of evapotranspiration can be made from pan-evaporation data using the following method from Doorenbos and Pruitt (1977):

$$E_g - C_{et}E_{\text{PAN}} \tag{12.25}$$

where E_g is the evapotranspiration calculated from pan evaporation, C_{et} is a coefficient relating pan evaporation to evapotranspiration, and E_{PAN} is pan evaporation. Values of C_{et} are presented in table 12.10. The coefficients shown in table 12.10 are given for two cases: **(1)** sites in cropped fields (Case A); and **(2)** sites in noncropped, dry-surface fields (Case B), as shown in figure 12.12. Jensen, Burman, and Allen (1990) state that adjustments are needed to relate to C_{et} for taller vegetation (such as alfalfa or tall grass), especially in hot, drier climates where crop height and aerodynamic roughness have a greater effect on E_g than in humid climates. For taller vegetation and aerodynamically rougher crops, the values of C_{et} are greater and vary less with differences in wind and relative humidity than do values for shorter, smoother grass surfaces.

In addition to the variation in coefficients with wind and relative humidity, there also is an interaction with radiation intensity (Jensen, Burman, and Allen 1990). The coefficients in table 12.10 apply to Class A pans, annually painted inside and out with aluminum paint, then mounted on a standard wooden platform so that the top of the pan is 40 cm above ground level. If pans are not well maintained or have been screened to protect them from birds or other animals, the coefficients need to be modified. For example, Jensen, Burman, and Allen (1990) recommend that pans with 12.5-mm mesh screen have coefficients increased by 5 to

TABLE 12.10 Suggested values of C_{et} for relating class-A pan evaporation to evapotranspiration from 8–15 cm tall, well-watered grass crop[1]

	Case A: Pan surrounded by short green crop				Case B: Pan surrounded by dry-surface gound[2]			
		Relative humidity (percent)[3]				Relative humidity (percent)[3]		
Wind speed (km/day)	Upwind fetch of green crop (m)	Low 20–40	Medium 40–70	High >70	Upwind fetch of dry fallow (m)	Low 20–40	Medium 40–70	High >70
Light	0	0.55	0.65	0.75	0	0.70	0.80	0.85
<170 km/day	10	0.65	0.75	0.85	10	0.60	0.70	0.80
	100	0.70	0.80	0.85	100	0.55	0.65	0.75
	1000	0.75	0.85	0.85	1000	0.50	0.60	0.70
Moderate	0	0.50	0.60	0.65	0	0.65	0.75	0.80
170–425 km/day	10	0.60	0.70	0.75	10	0.55	0.65	0.70
	100	0.65	0.75	0.80	100	0.50	0.60	0.65
	1000	0.70	0.80	0.80	1000	0.45	0.55	0.60
Strong	0	0.45	0.50	0.60	0	0.60	0.65	0.70
425–700 km/day	10	0.55	0.60	0.65	10	0.50	0.55	0.65
	100	0.60	0.65	0.70	100	0.45	0.50	0.60
	1000	0.65	0.70	0.75	1000	0.40	0.45	0.55
Very Strong	0	0.40	0.45	0.50	0	0.50	0.60	0.65
>700 km/day	10	0.45	0.55	0.60	10	0.45	0.50	0.55
	100	0.50	0.60	0.65	100	0.40	0.45	0.50
	1000	0.55	0.60	0.65	1000	0.35	0.40	0.45

[1] $E_a = C_{et} * E_{pan}$—Doorenbos and Pruitt 1974

[2] These coefficients apply only to conditions when the soil surface is indeed dry. Following rains for a day or two in midsummer and longer periods in the fall, winter, and spring, such pans are essentially equivalent to Case A type pans with large fetches. Rains also affect Case A type pans by essentially increasing the 0- and 10-meter fetch to an effective moist surface fetch of 1000 m or more. One large advantage of Case-B type pans is the minimal upkeep involved in siting of such a pan; that is, only an effective weed control program is needed for the site.

[3] Mean of maximum and minimum relative humidity

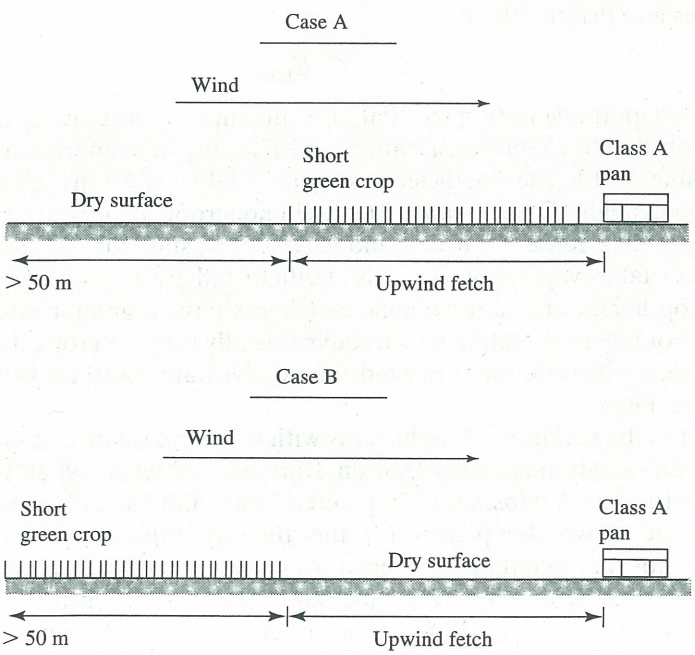

Figure 12.12 Schematic relating class-A pan evaporation to evapotranspiration (data from Jensen, Burman, and Allen 1990)

10 percent. If the pan is made of Monel metal, or is an old, unpainted, galvanized pan, coefficients need to decrease by 5 percent.

Change in Surface Storage

In water-balance calculations, surface storage can occur as ponds, reservoirs, or storage tanks that hold water temporarily or permanently, with and without seepage and/or evaporation losses. In a given time frame, water can enter or leave surface storage. The primary components of surface storage that are taken into account in the water-balance calculations are its water-surface elevation, surface area, and storage capacity. For a given storage reservoir, these components are usually lumped into a set of curves called elevation–area–capacity curves, as shown in figure 12.13. Such curves are easily constructed from the geometry of the storage reservoir, taken either from topographic maps or from prismatic shapes such as frustrums of regular pyramids or circular cones.

The factors that cause the reservoir storage to change include: precipitation falling directly on the reservoir; evaporation from the reservoir-water surface; inflow or outflow of ponded water; and seepage/infiltration from/to the reservoir. The elevation–area–capacity curve can also change over time if sediment is added to the reservoir through inflow, or is removed through natural or man-induced mechanisms.

Change in Soil-Moisture Storage

Change in soil-moisture storage is caused by precipitation falling on the soil surface, evaporation occurring directly from a wet-soil surface, evapotranspiration, and seepage/infiltration. The quantitative estimates of soil-moisture storage can be made using a running balance of soil-moisture storage as a "reservoir," subject to operating rules that describe when deep percolation (see figure 12.1) occurs, as well as the distribution of actual evapotranspiration with depth and currently available soil moisture. Typical operating rules related to retention

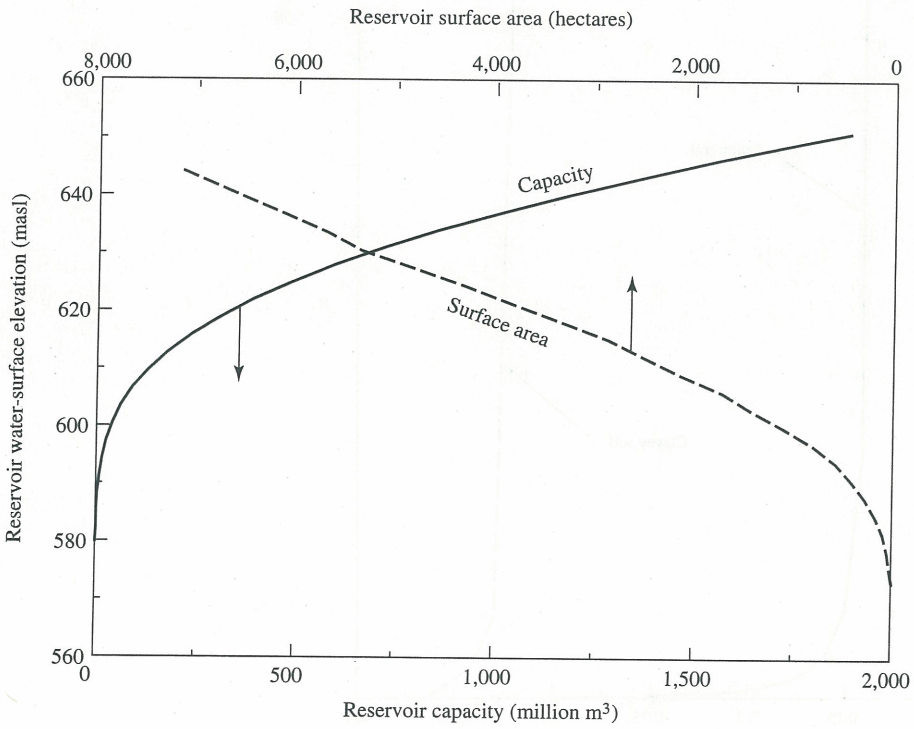

Figure 12.13 Typical elevation–area–capacity curves

(or movement) of soil moisture use the concepts of field capacity and permanent-wilting point. These two variables are generally defined as the volumetric-water content at matric potentials of approximately −340 and −15,300 cm of water, respectively, and are highly dependent upon soil texture. Figure 12.14 shows a typical relation between water content and matric potential for a sandy soil and a clay soil. Holtan et al. (1968), Rawls, Brakensiek, and Saxton (1982), and Rawls et al. (1993) provide soil-moisture versus matric-potential data for over 5,000 soils in the United States.

Operating rules in various soil-moisture balance calculations are proposed by Schroeder et al. (1994a, b). In simple water-balance models, soil moisture is allowed to move only if the water content exceeds field capacity. As shown on figure 12.1, the root-zone soil is often divided into several isotropic and homogeneous cells, whose soil properties are assumed to be uniform. Soil moisture is then moved from cell to cell at each time-step, until the water is evapotranspired or discharges from the lowermost cell as deep percolation. If the water content of the soil falls to permanent wilting point, then it is assumed that plants cannot extract moisture. This part of the soil-moisture rule is a lower bound on minimum soil moisture. If all pores are filled with water (saturation), then all additional water trying to enter the soil is assumed to run off.

Root-zone extraction of water by plants is not uniform with depth, because root densities usually decrease from near-ground surface to maximum rooting depth. Several models assume that water extraction from the soil by plant roots takes place in a linearly decreasing mode (Schroeder et al. 1994a, b; Davis and Neuman 1983). Kunkel and Murphy (1983) proposed that removal of water by plant roots is a parabolically decreasing function with depth, based upon test plot data.

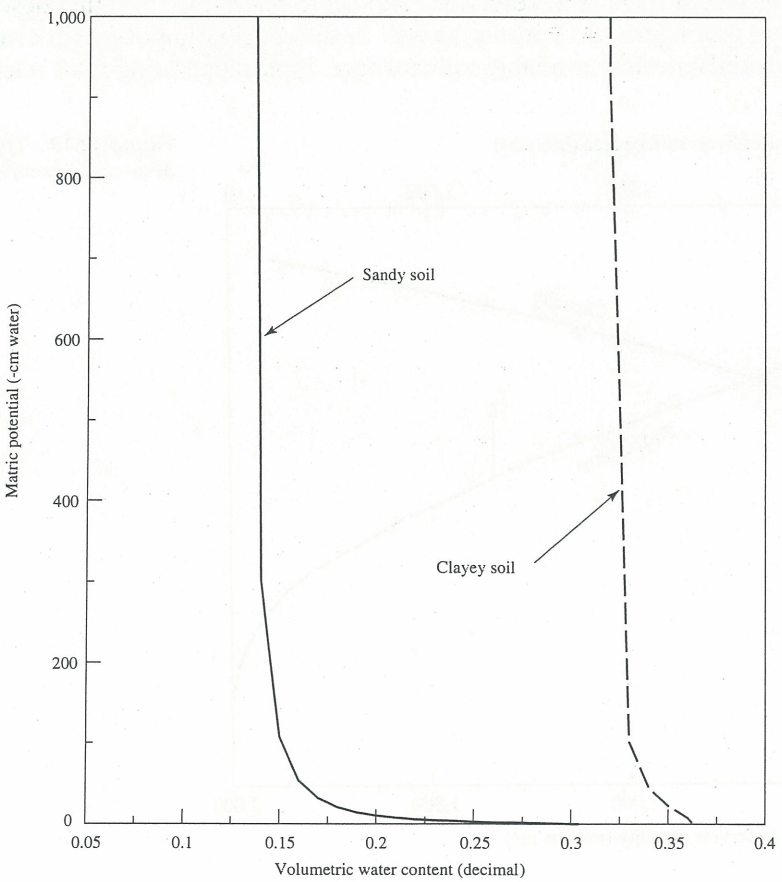

Figure 12.14 Typical soil-moisture characteristic curves

12.2 FIELD RADIATION AND ENERGY BALANCE

The radiation- and energy-balance equations can be derived exactly in the same manner as the water-balance equation. Radiation and energy are important because solar radiation is the primary external energy source that drives heat and water movement in the soil. Radiation includes various components of solar radiation such as incoming short-wave radiation, reflected short-wave radiation, and long-wave radiation. Energy components include—in addition to the radiation components—sensible and latent-heat fluxes from water and soil bodies (Rasmusson et al. 1993).

Radiation Balance

Averaged over the globe, the earth's surface absorbs approximately 124 kilolangleys (kly) (124,000 cal cm^{-2}) of solar radiation each year. Of this amount, approximately 52 kly yr^{-1} is radiated to the atmosphere from long-wave energy, and the remaining 72 kly yr^{-1} is the net radiation at the earth's surface (Sellers 1965). The earth's atmosphere absorbs only 45 kly yr^{-1} of solar radiation and radiates 117 kly yr^{-1} of long-wave energy; the net atmospheric radiation is -72 kly yr^{-1}. Thus, the atmospheric radiation losses (-72 kly yr^{-1}) exactly balance the earth's surface radiation gains (72 kly yr^{-1}), on the average (Sellers 1965). The surface net-radiation balance (or the net radiation) is given by

$$R_n = C_a + A_a - C_r - A_r + R_s(1 - a) - aR_s - R_b \tag{12.26}$$

This expression says that the radiation incident on a horizontal surface at the top of the atmosphere can be reflected and scattered back into space by clouds (C_r); by dry-air molecules, dust, and water vapor (A_r); or by the surface of the earth aR_s, where R_s is the sum of the direct (Q) and diffuse (q) solar radiation, respectively, incident on the earth's surface, and a is the surface albedo; and R_b is the effective outgoing radiation from the surface. Alternatively, this solar radiation can be absorbed by clouds (C_a); by dry-air molecules, dust, and water vapor (A_a); or by the earth's surface [$R_s(1 - a)$]. This radiation balance is shown schematically in figure 12.15.

As indicated in equation 12.18, direct and diffuse solar radiation can be estimated from cloudless-sky radiation (see table 12.7) and cloud cover. The effective outgoing radiation R_b can be estimated from the net long-wave radiation at the earth's surface. The net long-wave radiation is the sum of radiation being transmitted from the atmosphere to the earth, and from the earth to the atmosphere. Long-wave radiation is a function of the temperature of the radiating body. For both the atmosphere and the earth's surface—each with temperatures above absolute zero—the long-wave radiation R_b can be calculated using the radiation law:

$$R_b = \varepsilon\sigma T^4 \tag{12.27}$$

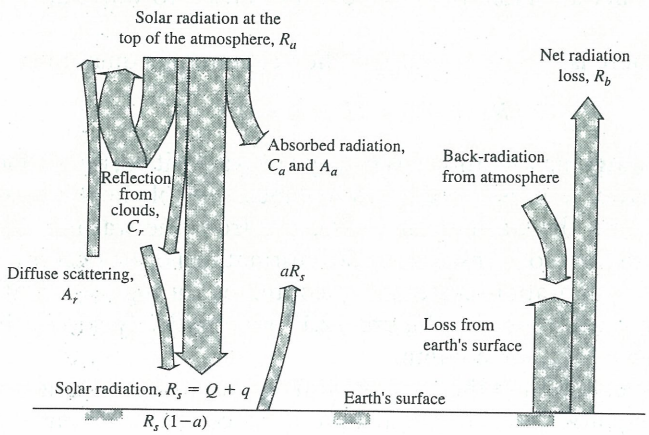

Figure 12.15 Schematic of the radiation balance at the Earth's surface (data from Sellers 1965 and Shuttleworth 1993)

where ε is emissivity (Stefan–Boltzmann constant), and T is the absolute temperature of the radiating body (273.2 + °C) (Kelvin). Values of the Stefan–Boltzmann constant are: $\sigma = 1.17 \times 10^{-7}$ cal cm^{-2} K^{-4} d^{-1} or $\sigma = 4.903 \times 10^{-9}$ MJ m^{-2} K^{-4} d^{-1}. Values of emissivity typical of surfaces on earth (water, snow, soil, vegetation) range from approximately 0.90 to 0.99. Typical values of emissivity can be found in Sellers (1965), or calculated by equations found in Jensen, Burman, and Allen (1990).

A portion of the solar radiation incident at the top of the atmosphere (R_a) reaches the ground (R_s). Typically, R_s is between 25 and 50 percent of R_a, whereas A_r is between 15 and 100 percent of R_s. Both of these values are influenced by albedo, which is typically 0.23 for land surfaces and 0.08 for water surfaces (Shuttleworth 1993).

Energy Balance

If one considers a soil or water column extending from the earth's surface to a depth where vertical heat exchange is negligible, the net rate, G, at which heat energy in this column is changing is equal to the sum of the rates at which heat energy is being added or lost by the various heat processes. The energy-balance equation at the earth's surface is given by

$$G = R_s(1 - a) + I_{\downarrow} - I_{\uparrow} - H - E + F_i - F_o \tag{12.28}$$

where $R_s(1 - a)$ is the heat added by absorption of solar radiation; $I_{\downarrow}$ is heat added by absorption of longwave counterradiation from the atmosphere; $-H$ is the heat added by downward transfer of sensible heat from the air, when the air is warmer than the soil or water surface; F_i is the horizontal transfer of heat into the soil or water column from the surroundings; $I_{\downarrow}$ is heat being lost by longwave radiation to the atmosphere; H is the transfer of sensible heat to the air if the air is cooler than the soil or water surface; E is the heat lost by evaporation (given by the product of mass of water evaporated times the latent heat of vaporization (590 cal g^{-1}); and F_o is the horizontal transfer of heat out of the column. These components are shown schematically on figure 12.16.

As indicated by equation 12.26, the first three terms of equation 12.28 are from the radiation balance R_n. The energy-balance equation is often written as

$$R_n = H + E + G + \Delta F \tag{12.29}$$

where $\Delta F = F_o - F_i$ is the net-subsurface flux of sensible heat out of a soil or water column. This flux is usually only important for large water bodies, where currents can transport considerable heat energy from one region to another. Over land, ΔF is negligible and

$$R_n = H + E + G \tag{12.30}$$

which implies that the net-available radiative energy is used to warm air, evaporate water, and warm the soil.

At night, when there is no solar radiation, the heat energy equation is

$$R_n = -I = H + E + G. \tag{12.31}$$

Because the effective outgoing radiation I is nearly always positive, the surface loses heat by radiation at night. In order to preserve the heat balance, sensible heat is usually transferred to the cooler surface from the warmer air ($-H$), and from the warmer deeper soil layers ($-G$). Negative evaporation (condensation or dew formation) often occurs also. However, in arid climates, positive evaporation customarily continues during the night, although at a much lower rate than during the day. Figure 12.17 schematically shows the daytime and nighttime energy balance for a soil column.

The heat-balance equation in the proper form applies over any time period. However, it is an approximate equation to the extent that small components have been neglected.

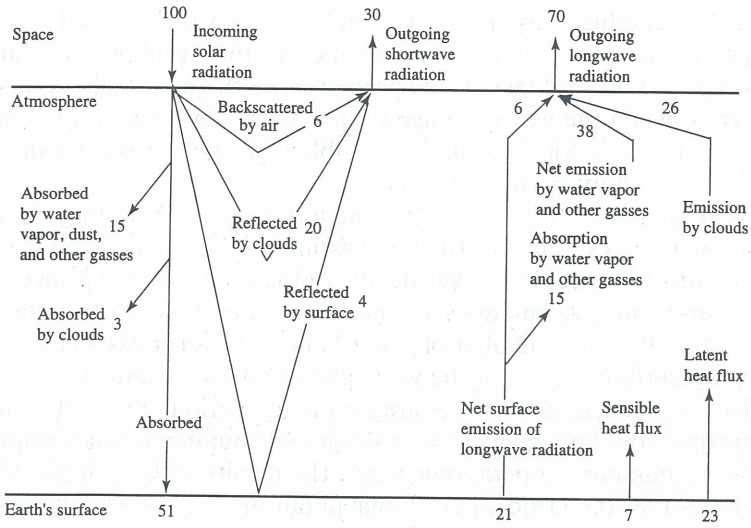

Figure 12.16 Schematic of the energy balance at the top of the atmosphere at the earth's surface; numbers indicate percentage of total incoming solar radiation (data from Rasmusson et al. 1993)

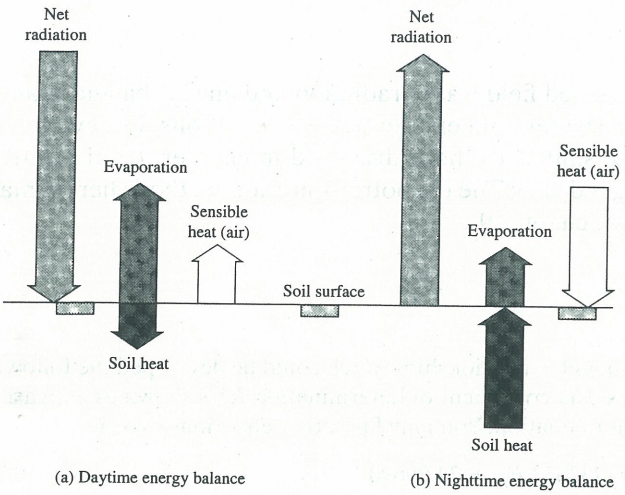

Figure 12.17 Schematic of daytime and nighttime energy balance (data from Rasmusson et al. 1993)

These might be important locally at a particular time, and include

- snowmelt, which may require approximately 10 ly d^{-1};
- dissipation of mechanical energy of wind, which can be between 1 and 10 ly d^{-1};
- heat transfer by precipitation, whose magnitude can reach 40 ly hr^{-1};
- expenditure of heat by photosynthesis, estimated at less than 5 percent of the incoming solar radiation, R_s;
- heat gain by biological oxidation processes such as forest fires, which can give off 850 ly d^{-1} of heat;
- other sources including combustion, volcanic eruptions, earthquakes, street lighting, and flux from the earth's interior.

12.3 WATER- AND ENERGY-BALANCE METHODOLOGY

The use of water balance for the sizing of water-storage ponds and reservoirs is often applied incorrectly. In order to have confidence that the water-storage facility is correctly sized according to the available hydrologic data, a traditional "once-through" use of the available

record is not acceptable. This "once-through" approach tries to find a "critical period" of wet or dry climatological or hydrological sequences that result in a maximum or minimum reservoir-volume or water-demand. The problem with this approach is that the designer does not likely know when the water-storage project comes on line, in relation to the historical hydrologic record. Therefore, not all the possible hydrologic cases nor operational cases for the water-storage facility are investigated.

To avoid this "once-through" pitfall, the following methodology for performing water and energy balances is stipulated. The basic assumption of letting the historical climatologic or hydrologic record repeat itself over the life of the water-storage project is still used. However, the water-balance calculations should begin in each year of the historic record. This method results in the same number of water-balance runs (or cases) as the number of years of hydrologic record. The data for the years prior to the start-date are transposed to the end of the project life cycle, so all analyses are for the full period of record. In this way, the initial project start-date could be in any year, resulting in a number of maximum or minimum values equal to the number of operational cases. The results of the sizing of water-storage facilities guarantees that the critical-period maximum or minimum required-reservoir volume are found for the period of record used.

SUMMARY

In this chapter we discussed field water, radiation and energy balances, and provided practical approaches to solve water- and energy-balance equations. The evapotranspiration methods in this chapter are similar to those discussed in chapter 9 and are frequently the ones used by the consulting industry. The evapotranspiration methods herein may be compared to the methods detailed in chapter 9.

ANSWERS TO QUESTIONS

12.1. Among the many possible relationships which could be developed the following were selected as potential predictors. The coefficient of determination R^2 is shown as a measure of the goodness-of-fit of the predictor equation. You may find other equations as well.

$$E_z = 0.7732072\,E_A + 34.09690 \qquad R^2 = 0.718 \qquad (12.32)$$

$$E_z = 1.0139667\,E_B - 50.01599 \qquad R^2 = 0.717 \qquad (12.33)$$

$$E_z = 0.4333176\,E_A + 0.561208\,E_B - 34.66132 \qquad R^2 = 0.799 \qquad (12.34)$$

$$E_z = 0.8920611\,E_A - 2.32 \times 10^{-4}\,(E_A)^2 - 20.269656 \qquad R^2 = 0.718 \qquad (12.35)$$

The nonlinear regression (equation 12.35) is not an improvement upon the linear regression shown in equation 12.32. Therefore, equations 12.32–34 constitute good predictors, but not the only ones, of the pan evaporation at Station Z. Additionally, because only three coincidental values were available at Station C, this station was not used in the regression analyses.

	Pan evaporation (mm)					Pan evaporation (mm)			
Date	Station A	Station B	Station C	Station Z	Date	Station A	Station B	Station C	Station Z
Jan-74	452.3				Jan-77	348.7	351.1		312.0
Feb-74	418.3				Feb-77	264.0	297.3		240.5
Mar-74	476.3				Mar-77		335.9		276.1
Apr-74	259.5				Apr-77	200.9	254.3		198.5
May-74	176.5				May-77	227.5	219.8		184.9
Jun-74	138.6				Jun-77	146.3	194.4	136.1	178.9

(*continued*)

Date	Pan evaporation (mm) Station A	Station B	Station C	Station Z	Date	Pan evaporation (mm) Station A	Station B	Station C	Station Z
Jul-74	164.5				Jul-77	172.5	238.1	199.5	135.9
Aug-74	197.0				Aug-77	195.2	260.1	200.1	166.0
Sep-74	260.5				Sep-77	241.6	335.0		256.2
Oct-74	334.5				Oct-77	317.4	303.5		308.7
Nov-74	371.0			128.1	Nov-77	357.5	363.8		326.4
Dec-74	373.6	340.3		255.7	Dec-77	358.2	399.6		359.5
Jan-75	342.4	303.1		188.4	Jan-78	349.9	390.7		319.5
Feb-75	247.5	263.9		102.9	Feb-78	263.8	305.5		289.1
Mar-75	290.7	267.8		199.0	Mar-78	217.2	381.1		318.9
Apr-75	239.4	215.8		226.0	Apr-78	193.6	272.8		236.6
May-75	162.8	166.4		140.0	May-78	181.5	255.0		184.4
Jun-75	129.8	148.3			Jun-78	175.1	216.5		121.6
Jul-75	143.4	157.2			Jul-78	138.1	199.8		135.3
Aug-75	197.3	201.2			Aug-78	188.8	230.4		190.3
Sep-75	245.7	240.8		228.0	Sep-78	235.1	242.0		217.3
Oct-75	341.7	317.3		239.3	Oct-78	319.6	266.1		314.4
Nov-75	344.8	328.7		316.6	Nov-78	346.1	282.6		279.6
Dec-75	361.0	339.4		367.1	Dec-78	391.0	336.7		334.2
Jan-76	301.0	297.7		227.0	Jan-79	377.4	348.6		265.9
Feb-76	293.0	268.1		230.4	Feb-79	317.6	332.0		276.1
Mar-76	295.0	287.2		337.8	Mar-79	320.8	364.1		287.0
Apr-76	232.4	248.8		128.1	Apr-79	222.0	312.9		196.0
May-76	180.7	174.1		132.3	May-79	148.7	244.4		185.5
Jun-76	121.3	169.8		127.7	Jun-79	124.8	221.2		133.1
Jul-76	158.9	177.4		120.4	Jul-79	153.1	267.1		168.1
Aug-76	176.2	191.1		136.7	Aug-79	184.5	268.5		205.0
Sep-76	258.5			206.2	Sep-79	263.8			219.5
Oct-76	322.8	294.4		244.5	Oct-79	299.0			284.2
Nov-76	352.2	324.1		324.4	Nov-79	308.5	288.8		
Dec-76	365.0	345.0		351.37	Dec-79	318.6	126.0		

ADDITIONAL QUESTIONS

12.2. The following table contains average annual values of precipitation and air temperature for various climatological stations at different elevations. Find a relation between average-annual precipitation and elevation, and annual-air temperature and elevation. Find the average annual precipitation and air temperature at elevation 3,000 meters above sea level (masl).

Station number	Elevation (meters asl)	Average annual precipitation (mm)	Average annual air temperature (°C)
1	3,750	—	4.1
2	5,150	—	−6.5
3	1,450	83.3	—
4	3,850	179.2	3.1
5	1,200	80.4	—
6	674	49.1	—
7	1,385	68.9	—
8	1,100	60.8	17.3
9	560	45.6	19.3
10	3,500	164.1	4.1
11	373	38.3	—

12.3. Use the various methods presented for calculation of evapotranspiration (Blaney–Criddle, Jensen–Haise, and pan-evaporation methods) to determine evapotranspiration in mm/day. Compare the results. Assume that the site is located in the southern hemisphere at latitude 40 °S and elevation 1,200 meters above sea level (366 feet) during the month of December. Further assume that the crop of interest is alfalfa. Mean climatological data for the site are given as follows.

Estimated atmospheric pressure = 887 mb
Mean maximum air temperature = 86 °F = 30 °C
Mean minimum air temperature = 53 °F = 11.7 °C
Mean air temperature = 69.5 °F = 20.8 °C

Mean dewpoint temperature = 49 °F = 9.4 °C
Mean vapor pressure = 11.8 mb
Mean wind movement at a height of 366 cm = 128 miles/day = 206 km/day
Mean relative humidity = 48%
Mean extraterrestrial solar radiation = 961 ly/day
Mean cloudless-day solar radiation = 740 ly/day
Mean observed solar radiation = 64 ly/day
Mean net radiation = 382 ly/day
Mean annual cloudless-sky radiation coefficient = 0.33
Mean cloud cover in tenths = 4

Estimated mean soil-heat flux = −6 ly/day
Mean Class A pan evaporation = 0.35 inches/day = 8.9 mm/day